High Power Laser Science and Engineering, (2023), Vol. 11, e14, 7 pages.
doi:10.1017/hpl.2022.45

HIGH POWER LASER SCIENCE AND ENGINEERING

RESEARCH ARTICLE

Short mid-infrared watt-level all-fiber nonlinear pulse compressor above 100-MHz pulse repetition rate

Jingcheng Shang[1,2], Chao Mei[4], Shengzhi Zhao[1], Yizhou Liu[1], Kejian Yang[2,3], Chun Wang[1], Tao Li[1,2,3], and Tianli Feng[1,2]

[1] *School of Information Science and Engineering, Shandong Provincial Key Laboratory of Laser Technology and Application, Shandong University, Qingdao, China*

[2] *Key Laboratory of Laser & Infrared System (Shandong University), Ministry of Education, Qingdao, China*

[3] *Institute of Novel Semiconductors, State Key Laboratory of Crystal Materials, Shandong University, Jinan, China*

[4] *Beijing Engineering and Technology Center for Convergence Networks and Ubiquitous Services, SCCE, University of Science and Technology Beijing, Beijing, China*

(Received 27 October 2022; revised 17 November 2022; accepted 19 December 2022)

Abstract

We firstly report a 2-μm all-fiber nonlinear pulse compressor based on two pieces of normal dispersion fiber (NDF), which enables a high-power scaling ability of watt-level and a high pulse compression ratio of 13.7. With the NDF-based all-fiber nonlinear pulse compressor, the 450-fs laser pulses with a repetition rate of 101.4 MHz are compressed to 35.1 fs, corresponding to a 5.2 optical oscillation cycle at the 2-μm wavelength region. The output average power reaches 1.28 W, which is believed to be the highest value never achieved from the previous 2-μm all-fiber nonlinear pulse compressors with a high pulse repetition rate above 100 MHz. The dynamic evolution of the ultrafast pulse inside the all-fiber nonlinear pulse compressor is numerically analyzed, matching well with the experimental results.

Keywords: few-optical-cycle pulses; high pulse repetition rate; nonlinear pulse compression

1. Introduction

The 2-μm ultrafast fiber laser has wide application fields, such as in gas detection[1], industrial material processing[2–4], medical surgery[5] and pumping mid-infrared (IR) optical parametric oscillators and optical parametric amplifiers[6,7]. At present, the research on 2-μm ultrafast fiber lasers is heading in the direction of generating much shorter laser pulses, particularly to the few-cycle pulse regime, which can be employed to drive a water-window X-ray desktop coherent light source[8] and realize attosecond light pulse generation[9]. By now, the shortest pulse duration of 45 fs (6.7 optical cycles) has been directly realized from a Tm-doped fiber oscillator, but with a low average output power of only 13 mW[10]. The average power can be scaled up with a chirped pulse amplifier, while with the cost of a broadened pulse duration that typically is hundreds of femtoseconds, which arises from the spectrum narrowing effect[11–16].

A fiber-based nonlinear pulse compressor, which relies on the nonlinear spectrum broadening process in the gas-filled hollow core fiber (HCF), Kagome-fiber or highly nonlinear fiber (HNLF), is the most efficient way to realize few-cycle laser pulses[17–19]. Among them, the HNLF possesses a large nonlinearity and can be employed for the compression of a small energy laser pulse with a high pulse repetition rate. Typically, the employed HNLF has a mode field diameter (MFD) either smaller than 4 μm or larger than 10 μm, both of which can be directly fused with standard single-mode fibers, and thus are favorable for constructing an all-fiber nonlinear pulse compressor without grating pairs or chirped mirrors for post pulse compression. Figure 1 summarizes the previously reported 2-μm all-fiber nonlinear pulse compressors. The shortest pulse duration of 13 fs (~2-cycle)[20] and highest output power of 24.5 W[21] have been realized with a large MFD-HNLF. However, the large MFD-HNLF requires a driving laser pulse at the microjoule level. A small MFD-HNLF is suitable for realizing the nonlinear pulse compression of a nanojoule-level laser pulse with a high pulse repetition rate above 100 MHz. For example, pulse durations of less than 40 fs with the repetition rate of more than or approximately 100 MHz have been realized

Correspondence to: Tianli Feng and Kejian Yang, School of Information Science and Engineering, Shandong Provincial Key Laboratory of Laser Technology and Application, Shandong University, Qingdao 266237, China. Email: tlfeng@sdu.edu.cn (T. Feng); k.j.yang@sdu.edu.cn (K. Yang)

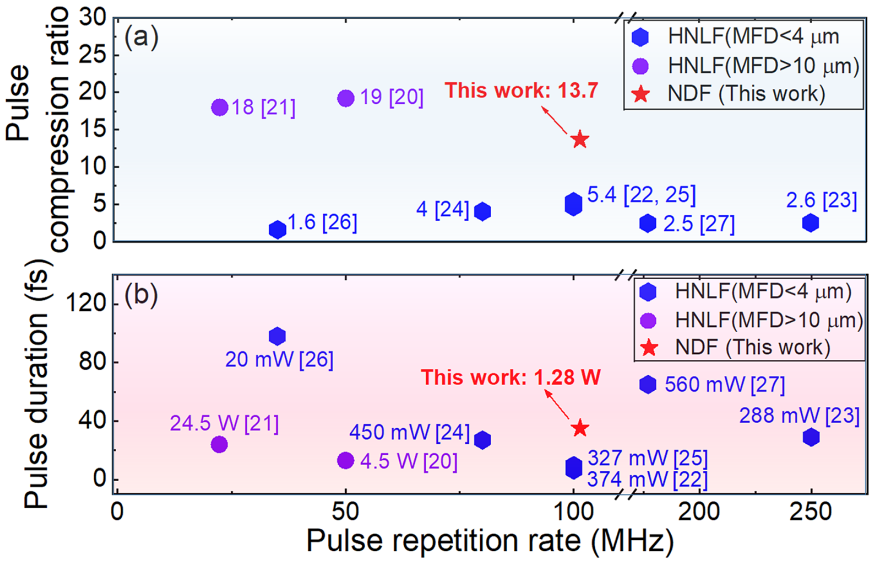

Figure 1. The reported 2-μm all-fiber nonlinear pulse compressors. (a) Pulse compression ratio versus pulse repetition rate. Label: the reported values of the pulse compression ratio. (b) Pulse duration versus pulse repetition rate. Label: the output average power. HNLF, highly nonlinear fiber; NDF, normal dispersion fiber; MFD, mode-field diameter; pulse compression ratio, the ratio between the driving laser pulse and the compressed laser pulse.

with small MFD-HNLF[22–25]. Few-cycle laser pulses with the repetition rate of more than 100 MHz are beneficial for improving the signal-to-noise ratio in spectroscopy experiments[26]. Besides that, such a pulse laser source also can be used for studying and controlling ultrafast charge transport in dielectrics[27] and in semiconductors[28].

The small MFD-HNLF typically has a large nonlinear coefficient of more than 10 W^{-1} km^{-1} and a total dispersion close to zero. The MFD of HNLF is much less than that of standard single-mode fiber (8 μm at 1950 nm). The large mode-mismatching between them increases the thermal load and optical loss at the position of the fusing point, which limits the further power scaling of small MFD HNLF-based nonlinear pulse compressors. Besides that, the pulse splitting effect usually shows up due to the overdriven nonlinearity with a high driving laser pulse power, thus making the average output power in small MFD HNLF-based nonlinear pulse compressors limited within several hundreds of milliwatt (see Figure 1(b)). The corresponding pulse compression ratios are less than 6 (see Figure 1(a)).

The 2-μm normal dispersion fiber (NDF) possesses a large normal dispersion of 0.137 ps^2/m and a moderate nonlinear coefficient of 2.68 W^{-1} km^{-1}, which is smaller than that of the HNLF of 10 W^{-1} km^{-1} but larger than that of the standard single-mode fiber of 0.53 W^{-1} km^{-1}. The input ultrafast laser pulse inside the NDF will be broadened in both the frequency and time domains, which lowers the peak power of the ultrafast laser pulse. This can prevent the pulse splitting effect induced by the overdriven nonlinearity and enable tolerating a higher driving laser power[29]. Simultaneously, considering the easy direct fusion of NDF with other standard single-mode fibers, it is very much expected to construct an all-fiber nonlinear pulse compressor. However, to the best of our knowledge, there is no report on an NDF-based all-fiber nonlinear pulse compressor at this moment.

In this paper, we develop an all-fiber nonlinear pulse compressor based on 2-μm NDF for the first time. A 450-fs long 2-μm laser pulse with a pulse repetition rate of 101.4 MHz is compressed to 35.1 fs, corresponding to 5.2 optical oscillation cycles. The pulse compression ratio is 13.7, which is more than two times larger than that of previously reported 2-μm all-fiber nonlinear pulse compressors operating in the high pulse repetition region of more than 100 MHz. The output average power exceeds 1 W, which is the highest average power never realized in previously reported 2-μm all-fiber nonlinear pulse compressors with a more than 100-MHz pulse repetition rate. The experimental results are further analyzed with the generalized nonlinear Schrödinger equation, showing good agreement with the simulated results.

2. Experimental results and discussion

Figure 2 presents a schematic diagram of the NDF-based all-fiber nonlinear pulse compressor. The ultrafast driving laser pulse is delivered from a Tm-doped fiber laser amplifier with a pulse repetition rate of 101.4 MHz (see Figure 3). The dispersion of the ultrafast laser pulse can be adjusted with a grating pair. The driving laser beam is collimated and fed into the following all-fiber nonlinear pulse compressor with a fiber collimator after transmitting through a half-wave plate. The pigtail of the input fiber collimator is a 19-cm long polarization maintaining fiber (PMF; Nufern, PM-SMF-10/130). Two pieces of NDFs (NDF1 and NDF2) with lengths of 28 and 15 cm are employed for nonlinear pulse compression. Between NDF1 and NDF2, a 40-cm long

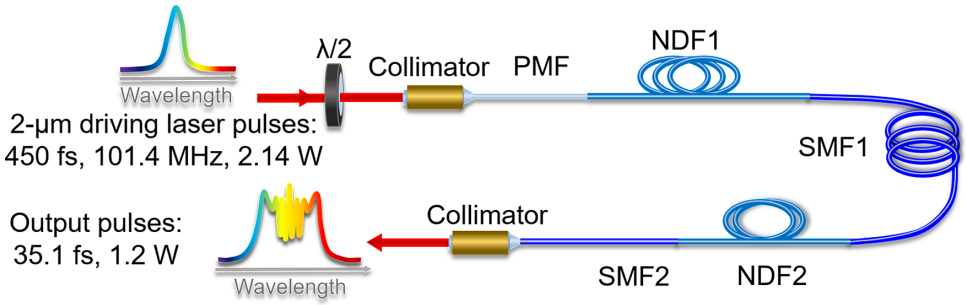

Figure 2. Schematic diagram of the NDF-based all-fiber nonlinear pulse compressor. λ/2, half-wave plate; PMF, polarization maintaining fiber; NDF, normal dispersion fiber; SMF, single-mode fiber.

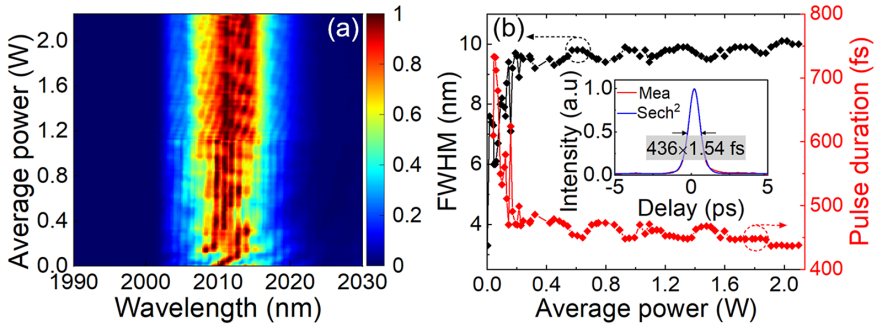

Figure 3. (a) The laser spectrum of the ultrafast driving laser pulse versus average power. (b) The full width at half maximum (FWHM) of the laser spectrum and pulse duration versus average power. Inset: the autocorrelation trace of the driving laser pulse at the maximum average power of 2.14 W.

single-mode fiber (Corning, SMF-28) is used to balance the NDF1- and self-phase modulation (SPM)-induced up-chirp. The laser pulses are coupled out by another fiber collimator with a 22-cm long single-mode pigtail (SMF2). The parameters of the employed fibers are listed in Table 1. The optical spectrum and the pulse duration of the laser pulse are respectively measured with a spectrometer (APE, WaveScan USB) and an autocorrelator (APE, pulseCheck). The output power is recorded with a power meter (Thorlabs, S425C).

Figure 3 shows the characteristics of the ultrafast driving laser pulse for different average output powers. As the average power scales up, the laser spectrum is always centered at 2012 nm with the range covering from 2000 to 2020 nm (see Figure 3(a)). Once the average power exceeds 0.4 W and further goes to 2.14 W, the spectral bandwidth keeps around approximately 10 nm (see Figure 3(b)). The pulse duration of the driving laser pulse approaches less than 500 fs when the output power exceeds 0.2 W. The measured autocorrelation trace at the maximum average power of 2.14 W shows the shortest pulse duration of 436 fs, which approaches the Fourier transform limited (FTL) value of 425 fs by assuming a sech^2 pulse shape.

Table 1. The parameters of the employed fibers in the 2-μm all-fiber nonlinear pulse compressor.

Fiber type	CD [a] (μm)	MFD [b] (ps^2/m)	GVD [c] (W^{-1} km^{-1})	γ [d]	NA [e]
PM-SMF-10/130	10	11	−0.095	0.37	0.15
SM2000D	2.1	4	0.137	2.68	0.37
SMF-28	8.2	9.2	−0.081	0.53	0.2

[a]CD: core diameter.
[b]MFD: mode field diameter.
[c]GVD: group velocity dispersion.
[d]γ is the nonlinear coefficient.
[e]NA: numerical aperture.

Initially, the ultrafast driving laser pulse is slightly stretched to 450 fs by introducing a positive group delay dispersion (GDD) of +18,000 fs^2. As the ultrafast driving laser pulse enters into the nonlinear pulse compressor, the up-chirped driving laser pulse can balance the polarization maintaining (PM) fiber-introduced anomalous dispersion of −18,000 fs^2, thus ensuring a near-FTL laser pulse reaches the NDF1. The laser spectrum out of the fiber NDF1 is broadened to a range of 200 nm from 1900 to 2100 nm (blue dashed line in Figure 4(c)), which is about 10 times broader than the ultrafast driving laser pulse. The 40-cm long single-mode fiber SMF1 behind NDF1 provides a negative GDD of −33,000 fs^2, which can partly compensate the up-chirp inside the ultrafast laser pulse. Then the laser pulse enters into the 15-cm long NDF (NDF2), which additionally adds a positive GDD of +20,000 fs^2. After passing through a 22-cm long single-mode fiber (SMF2) with a negative GDD of −17,800 fs^2, the ultrafast laser pulse is coupled out of the nonlinear pulse compressor with an output collimator.

Figure 4(b) shows the output power of the all-fiber nonlinear pulse compressor versus the input driving laser power.

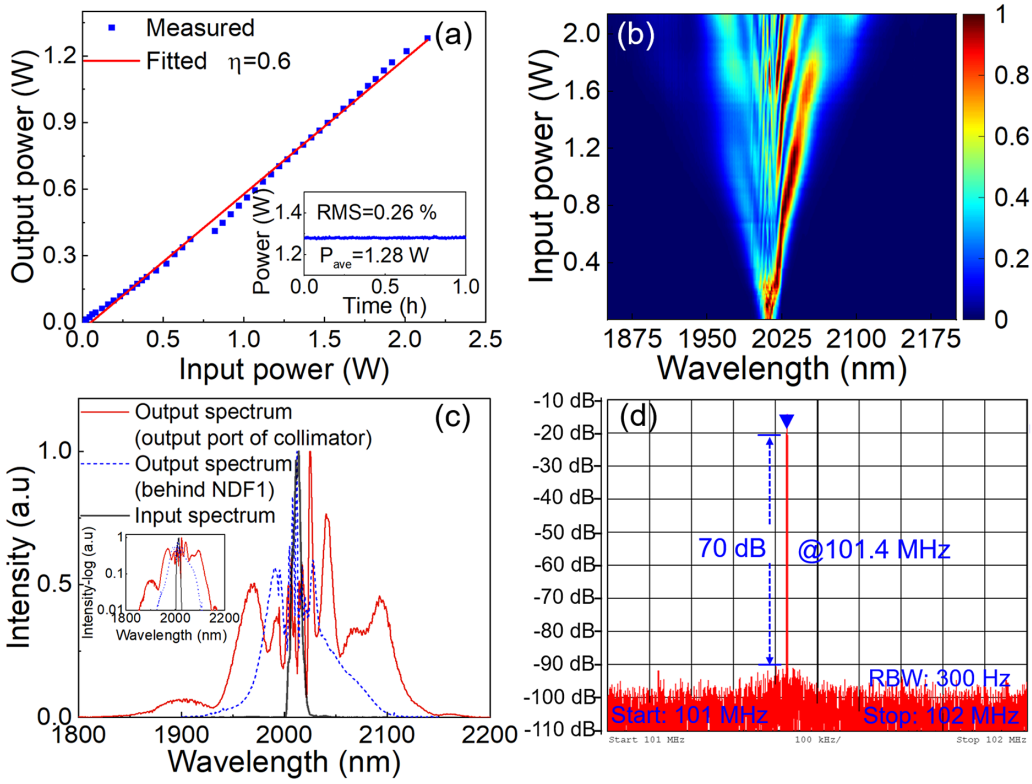

Figure 4. (a) The output power of the all-fiber nonlinear pulse compressor versus the driving laser power. Inset: the power stability at the maximum output power measured within 1 hour. (b) The measured spectrum output from the all-fiber nonlinear pulse compressor versus the driving laser power. (c) The output spectrum from the all-fiber nonlinear pulse compressor at the maximum output power of 1.28 W (red line), the output spectrum behind NDF1 (blue dashed line) and the input driving laser spectrum at the maximum power of 2.14 W (black line). (d) The radio frequency spectrum of the compressed laser pulse within the scanning range of 1 MHz with a resolution bandwidth (RBW) of 300 Hz.

As the average power of the ultrafast driving laser scales up to 2.14 W, the output power is linearly increased to 1.28 W with a power fluctuation of 0.26%. The corresponded power loss approaches approximately 40%, which mainly arises from the coupling loss (~8%) of the fiber collimator and the total mode-mismatching loss (~32%) of different fibers. With the increase of the input driving laser power, the nonlinear spectrum broadening effect is also enhanced (see Figure 4(b)). At the maximum output power, the output spectrum is extended to a spectral range of 300 nm from 1850 to 2150 nm, about 1.5 times larger than that measured behind NDF1 (see Figure 4(c)). The modulations on the top of the broadened spectrum are mainly attributed to the enhanced SPM effect and the PM fiber-induced birefringence filtering effect. The measured radio frequency spectrum shows a signal-to-noise ratio of 70 dB at 101.4 MHz. There are no obvious sub-peaks near the fundamental frequency comb, indicating that no strong pulse splitting effect occurs inside the all-fiber nonlinear pulse compressor.

Figure 5(a) gives the compressed pulse duration under different input powers. At the maximum input power, the measured autocorrelation trace is as presented in Figure 5(b). It shows that the shortest pulse duration is 35.1 fs by assuming a sech^2 pulse shape, corresponding to a pulse compression ratio of 13.7, which is believed to be the largest value never realized in a previously reported 2-μm all-fiber nonlinear pulse compressor operating with a more than 100-MHz pulse repetition rate (see Figure 1). The pedestal at the bottom of the autocorrelation trace arises from the higher order dispersion, which cannot be compensated with the single-mode fiber. The realized pulse duration is expected to be further narrowed with a shorter pulse duration and a higher peak power of the driving laser.

For further investigating the evolution of the ultrafast driving laser pulse inside the nonlinear pulse compressor, a numerical model is established based on the generalized nonlinear Schrodinger equation (GNLSE)[30], which is given as follows:

$$\frac{\partial A}{\partial z}+\frac{\alpha}{2}A+i\frac{\beta_2}{2}\frac{\partial^2 A}{\partial \tau^2}-\frac{\beta_3}{6}\frac{\partial^3 A}{\partial \tau^3} = i\gamma\left[|A|^2A+iS\frac{\partial}{\partial \tau}\left(|A|^2A\right)-R(t)A\frac{\partial}{\partial T}|A|^2\right]. \quad (1)$$

The right terms simultaneously incorporate the nonlinear effects, including SPM, self-steepening and the stimulated Raman scattering effect. In the GNLSE, A is the slowly varying pulse envelope, z represents the propagation distance, a

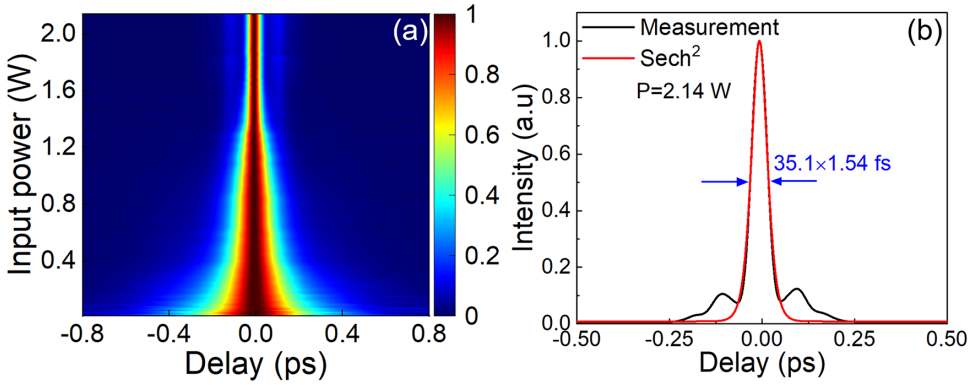

Figure 5. (a) The pulse duration of the compressed pulse versus input driving laser power. (b) The measured autocorrelation trace of the compressed laser pulse at the maximum input driving laser power of 2.14 W.

denotes the fiber loss, β_2 and β_3 are the second- and third-order dispersion parameters, respectively, ω_0 is the angular frequency of the driving laser pulse, T is the time delay relative to the driving laser pulse and γ is the nonlinear coefficient. Here, $S = \gamma_1(\omega_0)/\gamma(\omega_0)$ corresponds to the effect of self-steepening, where $\gamma_1(\omega) = \mathrm{d}\gamma(\omega)/\mathrm{d}\omega$ and ω_0 is the central angular frequency. The response function $R(t) = (1-f_R)\delta(t) + f_R h_R(t)$ includes both the instantaneous electronic and delayed Raman contributions, with $f_R = 0.18$ representing the fractional contribution of the delayed Raman response. For the Raman response function of the silica fiber, $h_R(t) = \tau_1\left(\tau_1^{-2} + \tau_2^{-2}\right)\exp(-t/\tau_2)\sin(t/\tau_1)$, in which τ_1 and τ_2 are 12.2 and 32 fs, respectively[31].

According to the parameters of the employed fibers in Table 1, we simulate the pulse and spectrum at the position between different types of fiber inside the nonlinear pulse compressor, which are presented in Figure 6. The center wavelength of the driving laser pulse is set to 2012 nm with a full width at half maximum (FWHM) bandwidth of 9.7 nm. The pulse duration is slightly up-chirped to 450 fs similar to that in the experiment (see Figures 6(a) and 6(g)). When the driving laser pulse firstly goes through the PMF, the laser pulse is shortened to 433 fs by the PMF-provided negative GDD of –18,000 fs^2 (see Figure 6(b)). The pulse spectrum slightly broadens from 9.7 to 10 nm (see Figure 6(h)). Once the laser pulse goes into the NDF (NDF1), the spectrum bandwidth broadens from 10 to 55 nm (see Figure 6(i)). Simultaneously, the laser pulse broadens from 433 to 615 fs, as shown in Figure 6(c). The laser pulse shows a parabolic shape, which is a typical characteristic of an ultrafast laser pulse propagating inside an NDF[32]. As the laser pulse further goes out of the single-mode fiber (SMF1), which provides a negative GDD of –33,000 fs^2, the laser pulse is compressed down to 180 fs (see Figure 6(d)). Simultaneously, the spectrum bandwidth further broadens to 67 nm (see Figure 6(j)). The narrowed laser pulse strengthens the nonlinear effect in the second NDF (NDF2), making the spectrum broaden to a range of 302 nm from 1811 to 2113 nm (see Figure 6(k)), which is about two times broader than that from NDF1. The pulse evolves into a parabolic shape with a pulse duration of 1040 fs, as shown in Figure 6(e). The residual chirp of the laser pulse is compensated with

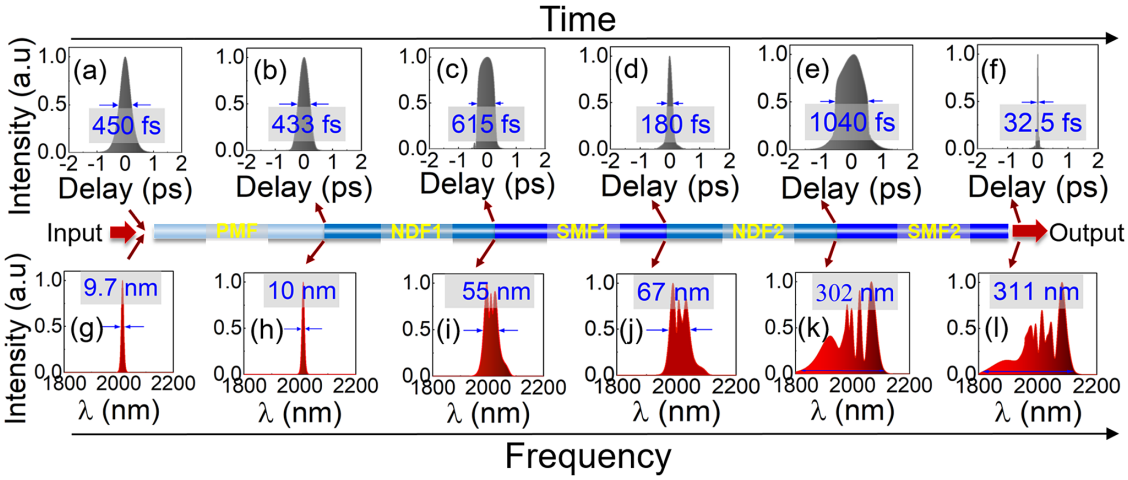

Figure 6. The simulated pulse (a)–(f) and spectrum (g)–(l) at the output port of each piece of fiber along the all-fiber nonlinear pulse compressor.

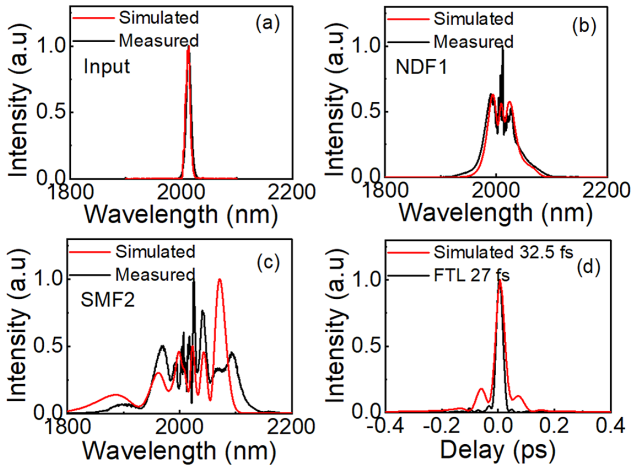

Figure 7. (a) The simulated (red line) and measured (black line) spectra of the ultrafast driving laser pulse. (b) The simulated (red line) and measured (black line) spectra at the output port of NDF1. (c) The simulated (red line) and measured (black line) spectra at the output port of SMF2. (d) The simulated and FTL pulses at the highest output power.

a second piece of single-mode fiber (SMF2) by providing a negative GDD of –17,800 fs^2, finally resulting in a pulse duration of 32.5 fs (see Figure 6(f)). Figure 6(l) is the final spectrum, which is slightly broadened to a range of 311 nm from 1814 to 2125 nm. Further calculation shows the peak power of the output pulse is 0.39 MW. The critical power of self-focusing can be estimated as $P_{cr} \approx \lambda^2/(2\pi n_0 n_2) =$ 22.6 MW, where $n_0 = 1.45$[33] and $n_2 = 1.94 \times 10^{-20}$ m^2/W[34] are the linear and nonlinear refractive indexes, respectively. Therefore, the pulse compression is completely induced by multiple compensation of the temporal chirp, and spatial effects make no contribution.

The simulated spectrum out of the first NDF (NDF1) matches well with the measured results (see Figures 7(a) and 7(b)). However, for the simulated spectrum out of SMF2, the intensity of the measured spectrum in the long wavelength region of more than 2050 nm is obviously lower than that of the simulation. This is attributed to the largely wavelength-dependent loss of the NDF, which is not considered in the simulation (Figure 7(c)). Besides that, the unaccounted PM fiber-induced birefringence filtering effect also results in a mismatching between the simulation and experiment. The red line in Figure 7(d) is the simulated 32.5 fs pulse, which approaches the FTL pulse of 27 fs (black line), corresponding to the residual GDD of +220 fs^2. The obvious pedestal at the bottom of the simulated single pulse (red line in Figure 7(d)) arises from the uncompensated high-order dispersion and the spectral shape of the simulated spectrum (red line in Figure 7(c)).

3. Conclusion

Based on the NDF, which possesses a moderate nonlinearity and large normal dispersion, we construct an all-fiber nonlinear pulse compressor. With the all-fiber nonlinear pulse compressor, 450 fs, 101.4 MHz, 2-μm ultrafast driving laser pulses are compressed to 35.1 fs with a pulse compression ratio of 13.7, corresponding to only 5.2 optical oscillation cycles. The average output average power is 1.28 W. Both the pulse compression ratio and the output average power are the state-of-the-art values never achieved from previously reported more than 100-MHz 2-μm all-fiber nonlinear pulse compressors. Both the experiment and theory show that the NDFs are suitable for nonlinear pulse compression of 2 μm high-power laser pulses.

Acknowledgements

This work was supported by the National Natural Science Foundation of China (Nos. 62005144, 61775119, and 62175128); the Natural Science Foundation of Shandong Province (No. ZR2020QF096); the Qilu Young Scholar Program of Shandong University; the Taishan Scholar Foundation of Shandong Province (No. tsqn201812010); and the High-level Talent Cultivation Funds of the State Key Laboratory of Crystal Materials of Shandong University.

References

1. A. Pal, S. Y. Chen, R. Sen, T. Sun, and K. T. V. Grattan, Laser Phys. Lett. **10**, 085101(2013).
2. B. Voisiat, D. Gaponov, P. Gečys, L. Lavoute, M. Silva, A. Hideur, N. Ducros, and G. Račiukaitis, Proc. SPIE **9350**, 935014 (2015).
3. J. Geng, X. Fang, L. Zhang, G. Yao, L. Xu, F. Liu, W. Tang, L. Shi, and M. Qiu, Light Adv. Manuf. **2**, 274 (2021).
4. J. Geng, W. Yan, L. Shi, and M. Qiu, Light Sci. Appl. **11**, 189 (2022).
5. N. M. Fried and K. E. Murray, J. Endourol. **19**, 31 (2005).
6. Q. Fu, L. Xu, S. Liang, P. C. Shardlow, D. P. Shepherd, S. Alam, and D. J. Richardson, Opt. Express **28**, 5741 (2020).
7. W. Yao, Y. Wang, S. Tomilov, M. Hoffmann, S. Ahmed, C. Liebald, D. Rytz, M. Peltz, V. Wesemann, and C. J. Saraceno, Opt. Express **30**, 41075 (2022).
8. T. Popmintchev, M. C. Chen, D. Popmintchev, P. Arpin, S. Brown, S. Ališauskas, G. Andriukaitis, T. Balčiunas, O. D. Mücke, A. Pugzlys, A. Baltuška, B. Shim, S. E. Schrauth, A. Gaeta, C. Hernández-García, L. Plaja, A. Becker, A. Jaron-Becker, M. M. Murnane, and H. C. Kapteyn, Science **336**, 1287 (2012).
9. C. Zhang, G. Vampa, D. M. Villeneuve, and P. B. Corkum, J. Phys. B **48**, 061001 (2015).
10. Y. Nomura and T. Fuji, Opt. Express **22**, 12461 (2014).
11. Z. Ren, F. Slimen, J. Lousteau, N. White, Y. Jung, J. H. V. Price, D. J. Richardson, and F. Poletti, Opt. Lett. **46**, 3013 (2021).
12. A. Rampur, Y. Stepanenko, G. Stępniewski, T. Kardaś, D. Dobrakowski, D. M. Spangenberg, T. Feurer, A. Heidt, and M. Klimczak, Opt. Express **27**, 35041 (2019).
13. P. Wan, L. Yang, and J. Liu, Opt. Express **21**, 21374 (2013).
14. R. Chen, J. Yang, X. Qi, J. Xu, and Y. Tang, Acta Photonica Sinica **45**, 1023001 (2016).
15. S. Dong, G. Chen, X. Wang, L. Yu, W. Zhao, and Y. Wang, Acta Photonica Sinica **33**, 073132 (2004).

16. R. Chen, Y. Xing, Y. Zhang, J. Wang, Z. Wei, and G. Chang, Acta Photonica Sinica **51**, 0751415 (2022).
17. E. A. Khazanov, S. Y. Mironov, and G. Mourou, Usp. Fiz. Nauk **189**, 1173 (2019).
18. K. Murari, G. Cirmi, H. Cankaya, G. J. Stein, B. Debord, F. Gérôme, F. Ritzkosky, F. Benabid, O. Muecke, and F. X. Kärtner, Photon. Res. **10**, 637 (2022).
19. M. Nisoli, S. De Silvestri, and O. Svelto, Appl. Phys. Lett. **68**, 2793 (1996).
20. T. P. Butler, D. Gerz, C. Hofer, J. Xu, C. Gaida, T. Heuermann, M. Gebhardt, L. Vamos, W. Schweinberger, J. A. Gessner, T. Siefke, M. Heusinger, U. Zeitner, A. Apolonski, N. Karpowicz, J. Limpert, F. Krausz, and I. Pupeza, Opt. Lett. **44**, 1730 (2019).
21. C. Gaida, M. Gebhardt, F. Stutzki, C. Jauregui, J. Limpert, and A. Tünnermann, Opt. Lett. **40**, 5160 (2015).
22. S. Xing, D. M. B. Lesko, T. Umeki, A. J. Lind, N. Hoghooghi, T. H. Wu, and S. A. Diddams, APL Photonics **6**, 0086110 (2021).
23. J. Wang, W. Lai, K. Wei, K. Yang, H. Zhu, Z. Zheng, C. Guo, S. Ruan, and P. Yan, Opt. Lett. **46**, 2445 (2021).
24. R. Herda and A. Zach, in *Photonics Conference (IPC)* (IEEE, 2013).
25. S. Xing, A. S. Kowligy, D. M. B. Lesko, A. J. Lind, and S. A. Diddams, Opt. Lett. **45**, 2660 (2020).
26. P. R. Griffith and J. A. De Haseth, Science **222**, 297 (1983).
27. A. Schiffrin, T. Paasch-Colberg, N. Karpowicz, V. Apalkov, D. Gerster, S. Mühlbrandt, M. Korbman, J. Reichert, M. Schultze, S. Holzner, J. V. Barth, R. Kienberger, R. Ernstorfer, V. S. Yakovlev, M. I. Stockman, and F. Krausz, Nature **493**, 70 (2013).
28. O. Schubert, M. Hohenleutner, F. Langer, B. Urbanek, C. Lange, U. Huttner, D. Golde, T. Meier, M. Kira, S. W. Koch, and R. Huber, Nat. Photonics **8**, 119 (2014).
29. N. Raabe, T. Feng, T. Witting, A. Demircan, C. Brée, and G. Steinmeyer, Phys. Rev. Lett. **119**, 123901 (2017).
30. E. M. E. Zayed and A. Al-Nowehy, Eur. Phys. J. Plus **132**, 475 (2017).
31. Q. Lin and G. P. Agrawal, Opt. Lett. **31**, 3086 (2006).
32. I. A. Sukhoivanov, S. O. Iakushev, O. V. Shulika, A. Díez, and M. Andrés, Opt. Express **21**, 17769 (2013).
33. R. Kitamura, L. Pilon, and M. Jonasz, Appl. Opt. **46**, 8118 (2007).
34. G. N. Patwardhan, J. S. Ginsberg, C. Y. Chen, M. M. Jadidi, and A. L. Gaeta, Opt. Lett. **46**, 1824 (2021).